Algal Research 97 (2026) 104775

Contents lists available at ScienceDirect

Algal Research

journal homepage: www.elsevier.com/locate/algal

Attenuated levels of solar UVA enhance inorganic carbon acquisition and assimilation with mitigation of oxidative damages in *Pyropia yezoensis*

Di Zhang [a,*], Nannan Sun [a], Yonglong Xiong [b], Kunshan Gao [b,c,**]

[a] School of Ocean, Yantai University, China
[b] State Key Laboratory of Marine Environmental Science, College of Ocean and Earth Sciences, Xiamen University, China
[c] Co-Innovation Center of Jiangsu Marine Bio-industry Technology, Jiangsu Ocean University, China

ARTICLE INFO

Keywords:
Antioxidant enzymes
Carbonic anhydrase
CO_2 concentrating mechanism
Photosynthesis
Pyropia yezoensis
Ultraviolet radiation

ABSTRACT

The commercially important red macroalga *Pyropia yezoensis* is naturally exposed to high levels of both photosynthetically active and ultraviolet radiation (PAR and UVR) either in its habituated upper intertidal zones or farmed areas. While both UVA and UVB levels around noon are known to inhibit photosynthesis and growth of *P. yezoensis*, here we show that attenuated levels (by about 70%) of solar radiation led to either none or stimulated effects on its photosynthetic performance in the absence of UVB, with UVA enhanced the activity of carbonic anhydrase (CA) and upregulated carbon concentrating mechanisms (CCMs), leading to sustained photochemical yield (F_v/F_m) and net photosynthetic rate. While addition of UVB decreased the yield and net photosynthesis and exacerbated photorespiratory carbon loss, along with the activity of Rubisco was significantly suppressed. Such attenuated levels of UVA played a role in protecting the photosynthetic electron transport chain from over-reduction and minimizing the formation of ROS, while UVB induced photodamage and oxidative stress, as reflected by the decreased F_v/F_m and the increased contents of reactive oxygen species (ROS) and malondialdehyde (MDA). Transcriptomic data supported these physiological changes, with upregulated genes (e.g., *tktA*, *FBP*, *GAPDH*, *can*, *cah*) in the presence of UVA, while addition of UVB downregulated genes related to light-harvesting and photosystem repair. In conclusion, attenuated levels of solar UVA act as a beneficial signal for the red alga to optimize carbon fixation, implying that *P. yezoensis* farmed at deeper depths or under cloudy weathers benefit from solar UVA, where UVB can penetrate to much lesser depths.

1. Introduction

Intertidal macroalgae, especially those distributed at upper zones, are exposed to high levels of incident solar radiation with UVA (315–400 nm) and UVB (218–315 nm) in addition to photosynthetically active radiation (PAR, 400–700 nm). Effects of UVR (UVA + B) have been reported to be divergent on marine primary producers, including macroalgae [1–4]. High levels of UVA significantly inhibit both photosynthesis and growth of *Gracilaria lemaneiformis* [5] and *Corallina sessilis* [6], while moderate levels of UVA benefitted the growth of *Fucus gardneri* [7] and *Pyropia haitanensis* [8], as well as some other macroalgae [9]. In terms of UVB, it usually causes negative effects to macroalgae, such as decreasing the contents of phycobiliproteins and Chl*a* in *Kappaphycus alvarezii* [10], damaging DNA, proteins and/or lipids [11] and harming photosynthetic apparatus, lowering photosynthesis in *Gracilaria lemaneiformis* and *Ulva prolifera* [12,13]. Moreover, UVB exposure can also inhibit the synthesis of carotenoids, e.g., lutein and zeaxanthin [14–16], further decreasing the heat dissipation and exacerbating photoinhibition, resulting in an accumulation of reactive oxygen species (ROS) [17].

Pyropia (also known as *Porphyra*, *Neopyropia*) (Rhodophyta), an economically important marine crop worth ~US$0.95 billion per year [18], has been widely farmed in both China and other Asian countries. Incident noon levels of UVR negatively affected the photosynthesis and growth of *Pyropia yezoensis*, with a significant occurrence of photoinhibition [19,20]. UVR can directly induce pigment photobleaching, PSII proteins degradation, reduce enzymes' activity involved Calvin cycle, and directly or indirectly cause DNA damages in macroalgae [2]. Recent works demonstrated that UV-absorbing compounds, non-photochemical quenching (NPQ), as well as cyclic electron transport

* Corresponding author.
** Correspondence to: K. Gao, State Key Laboratory of Marine Environmental Science, College of Ocean and Earth Sciences, Xiamen University, China.
E-mail addresses: zhangdi@ytu.edu.cn (D. Zhang), ksgao@xmu.edu.cn (K. Gao).

https://doi.org/10.1016/j.algal.2026.104775
Received 19 November 2025; Received in revised form 3 April 2026; Accepted 29 May 2026
Available online 2 June 2026

around photosystem I (PSI) were up-regulated to absorb and/or dissipate to relief the photodamages [19,20]. While photoinhibitory effects of UVA and UVB are well-documented, their impacts on the downstream processes, particularly carbon acquisition and enzyme activities in *Pyropia*, remains less explored, though UVA was shown to play an important role in its germination and morphogenesis [8].

Due to the low diffusion rate and solubility of CO_2 in seawater, coupled with the low affinity and catalytic efficiency of Rubisco, macroalgae have evolved unique CO_2 concentration mechanisms (CCMs) to overcome carbon limitation [21]. Since inorganic carbon acquisition is the prerequisite for carbon assimilation, which is the main photosynthetic electron sink, functionality of CCMs under different levels of UVA and UVB needs to be investigated for macroalgae, especially for the economically important *Pyropia* spp.. It has been documented that exposures to UVR affect the CO_2 concentrating mechanisms (CCMs) in diatoms [22], with moderate levels of UVA stimulating the activity of periplasmic carbonic anhydrase in the diatom *Skeletonema costaum* [23]. Such UV-induced effects on the CCMs seem dependent on exposure time span [24]. In *P. yezoensis*, UVR-induced photosynthetic inhibition is alleviated under elevated CO_2 [19,20], little is known how the exposures to UVR would affect its CCMs. Here, we hypothesize that interplay between photosynthesis, CCM regulation, light stress, and antioxidant enzymes activity in *Pyropia* spp. can be affected by UVR, the extent or direction of the effects would depend on doses or intensity of UVA or UVB. To test this, we grew *P. yezoensis*, under incident solar radiation with or without UVR, and investigated the functionality of CCMs, UVR-induced oxidative damages and transcriptomic responses in *P. yezoensis* to UVA and UVB.

2. Material and methods

2.1. Experimental treatments and measurements of UV irradiances

Thalli of *Pyropia yezoensis* were collected from rafts offshore of Lianyungang, Jiangsu Province, China, on December 2023, and transported to the laboratory in a cooled Styrofoam box. Following rinsing, thalli of ~0.1 g fresh weight were grown for two weeks in 2 L quartz tubes filled with natural seawater without a separate acclimation period, which were placed diagonally (with the upper end open to air) in a flow-through water bath outdoors, exposed to natural solar irradiance. The temperature was maintained at 9 ± 1 °C, which corresponded to the in situ seawater temperature at the collection site and was consistent with previous experimental studies [19,20]. The experiment was conducted from 2 to 16 December under natural photoperiod and irradiance fluctuations, seawater was changed every 2–3 days. The seawater in each tube was continuously aerated (300 mL per min) with an air pump. Thalli were exposed to irradiances above 400 nm (PAR alone), 315 nm (PAR + UVA) and 280 nm (PAR + UVR) by covering the quartz tubes with JB400 glass filter, ZJB320 glass filter, or ZJB280 glass filter (Nantong Yinxing Optical CO., LTD, China), respectively (Fig. S1).

The incident solar irradiances were continuously monitored and recorded per minute by a broadband solar radiometer (EKO Instruments Co., LTD, Japan). The maximal and daily average PAR values during the experimental period were 957.6 ± 85.4 and 215.3 ± 45.3 μmol photons m^{-2} s^{-1}, respectively, the corresponding values for UVA were 11.3 ± 1.2 and 2.5 ± 0.6 W m^{-2}, and 0.4 ± 0.05 and 0.1 ± 0.02 W m^{-2} for UVB. Due to the shade effect induced by trees near the cultivation area, ~30% of the recorded light intensity was attenuated from ~12:00 am, as measured with a PAR sensor equipped in Dual-PAM-100 (Walz, Effeltrich, Germany). The spectral irradiance of natural sunlight was obtained from a clear day using a spectroradiometer (QE65000 with Spectrasuite operating software and OmniDriver, Ocean Optics) over 250–800 nm with 1 nm resolution. For each treatment, the spectral irradiance reaching the thalli was obtained by multiplying the measured spectrum by the filter transmittance (ideal step function: 1 for λ ≥ cut-off, 0 otherwise) and by the shading attenuation factor of 0.7. The biologically effective weighted irradiance for photoinhibition was calculated as:

$$E_{photoinhibition/DNA} = \sum_{\lambda=280}^{400} E(\lambda) \times T(\lambda) \times A_{photoinhibition/DNA}(\lambda) \times \Delta\lambda$$

where $E_{photoinhibition/DNA}$ is the weighted irradiance for photoinhibition/DNA, E(λ) is the spectral irradiance, T(λ) is the filter transmittance and A_{photo} (λ) is the action spectrum of [25,26]. Numerical integration was performed using the trapezoidal rule with 1 nm intervals. The resulting values are presented in Table 1.

After two weeks of cultivation, the fresh weight of thalli in each tube increased to over 0.5 g, and with two independent batches, a total of >1 g fresh weight per treatment was collected for subsequent analyses. In addition, thalli used for non-destructive measurements (e.g., chlorophyll fluorescence and gas exchange) were collected and re-used for biochemical assays, ensuring sufficient biological material for all analyses. Measurements of photochemical activities and carbon utilizations were carried out on the end of day at 10:00–14:00. A total of 9 tubes containing different individual thalli were used for measurements of each parameter. Meanwhile, fresh samples used for the analysis of Rubisco activity, reactive oxygen species (ROS) content, MDA content, SOD and CAT activities, were quickly frozen with liquid nitrogen and stored at −80 °C until analysis. All physiological parameters were expressed on a fresh weight basis.

2.2. Measurements and analyses of chlorophyll fluorescence and gas exchange

A Dual-wavelength pulse-amplitude modulated (PAM) fluorescence monitoring system (Dual-PAM-100, Walz, Effeltrich, Germany) was applied to measure the maximum quantum yield (F_v/F_m). The minimal fluorescence (F_o) of 20 min dark-acclimated thalli was induced by a pulsed red measuring light of ~0.2 μmol photons m^{-2} s^{-1}, and the maximum fluorescence (F_m) was measured following a 0.8 s saturating flash (~5000 μmol photons m^{-2} s^{-1}). The maximum quantum yield of PSII was calculated as:

$$Fv/Fm = (Fm - Fo)/Fm$$

A GFS-3000 gas exchange system (Walz, Effeltrich, Germany) was employed to measure the net photosynthesis rates, the respiration rates, as well as the photosynthesis versus CO_2 curves (PC curves). Net photosynthesis rates (Pn) and respiration rates were evaluated with the difference in CO_2 concentrations of influx and efflux to and from the chamber (μatm) under light (~200 μmol photons m^{-2} s^{-1}) and dark conditions, respectively. The Pn and respiration rates were calculated according to Von Caemmerer and Farquhar [27] as follows:

$$\mathrm{Pn}\Big/\text{respiration rates} = \Delta C \times F \times 60 \times \frac{273}{(273 + T) \times 22.4 \times FW}$$

where ΔC represents the difference in CO_2 concentrations of influx and efflux of the chamber (μatm), F is the gas flow rate, 500 μmol min^{-1}, with conversions based on the molar volume of gas at standard atmospheric pressure (22.4 L mol^{-1}), T the temperature inside the chamber (°C) and FW the fresh weight of algal thalli (g). PC curves were evaluated with changes of Pn under six incremental external aerial CO_2 concentrations, 60, 200, 500, 800, 1500, 2000 μatm. The relative air humidity and the temperature were 80% and 10 °C, respectively, and the actinic light were ~ 200 μmol photons m^{-2} s^{-1}. The maximal photosynthetic rate V_{max} (μmol CO_2 g^{-1} FW h^{-1}) and the half-saturation constant ($k_{0.5}$, μatm) were obtained by fitting Pn at various CO_2 concentrations with the Michaelis-Menten formula.

Table 1
Irradiance parameters under each treatment condition. PAR values (μmol photons m^{-2} s^{-1}) and UV (UVA and UVB, W m^{-2}) were measured at rooftop (EKO radiometer) and then multiplied by a shading attenuation factor of 0.7 to estimate the irradiance reaching the thalli. Average daily doses (kJ m^{-2}) were calculated by multiplying the irradiance by the photoperiod (supposed to be 10 h, 36,000 s) and converting to kJ (×0.001). Weighted irradiances for photoinhibition and DNA damage (W m^{-2}) were obtained by numerical integration (280–400 nm, 1 nm intervals) of the product of: (i) the measured solar spectral irradiance (Fig. S2) after applying the filter cut-off (ideal step function: 1 for λ ≥ cut-off, 0 otherwise) and the 0.7 attenuation factor; (ii) the action spectrum of Jones & Kok (1966) for photoinhibition or Setlow (1974) for DNA damage; and (iii) the wavelength interval (1 nm). The integration was performed using the trapezoidal rule. Values are presented as average values recorded during the experiment. "–" indicates not applicable.

Treatment	PAR	UVA	UVB	Average daily PAR dose	Average daily UVA dose	Average daily UVB dose	Weight irradiance (photoinhibition)	Weight irradiance (DNA damage)
PAR	150.7	–	–	5425	–	–	0	0
PAR + UVA	150.7	1.75	–	5425	63.0	–	0.18	<0.01
PAR + UVA + UVB	150.7	1.75	0.07	5425	63.0	2.52	0.27	0.11

2.3. Measurements of carbonic anhydrase activity

The carbonic anhydrase (CA) activity was determined according to the method described by Giordano and Maberly [28]. About 0.1 g thalli were cut into small pieces and placed in a centrifuge tube with 5 mL CO_2-free seawater at pH 8.2 and 4 °C. Following the addition of 2 mL of ice-cold CO_2-saturated ddH_2O, the duration time for the pH of solution to decrease from 8.2 to 7.2 was recorded. The relative enzyme activity (REA) of $CA_{periplasmic}$ is calculated as:

$$REA = \left(\frac{T_0}{T} - 1\right) \times 10$$

where T_0 and T were the time required in the reaction without and with *P. yezoensis*. Following the measurements of $CA_{periplasmic}$, the used thalli was ground with liquid nitrogen and the total activity of CA was measured in the same way as above.

2.4. Measurements of photorespiration rates

A PreSens Microx 4 oxygen meter (PreSens, Regensburg, Germany) was employed to measure the photorespiration, which was estimated by calculating the difference in net photosynthetic oxygen evolution between low (2%) and ambient (21%) O_2 levels [13,29].

2.5. Measurements of reactive oxygen species, MDA Contents, antioxidant enzymes and Rubisco enzymes activities

Fresh samples were ground with liquid nitrogen and the tissue homogenates were used to analyze the ROS, MDA contents, SOD, CAT enzyme (Jiancheng, Nanjing, China) and Rubisco (Keming, Suzhou, China) activities of *P. yezoensis* following the manufacturer's protocols. Detailed procedures for measurements are provided in the supplementary material.

2.6. Transcriptome sequencing

Transcriptome sequencing was carried out by Genedenovo Biotechnology Co., Ltd. (Guangzhou, China). The total data volume of the transcriptome sequencing is 29.3 GB. After the culture, the total RNA was extracted from fresh thalli in the 0.1 μM treatment group using TRIzol (Invirogen, Carlsbad, CA, USA). The purity and integrity of RNA were assessed on a Nanophotometer spectrophotometer and an Agilent 2100 bioanalyzer (Agilent Technologies, Palo Alto, CA, USA). The qualified samples were selected to build cDNA library. Before analysis, the raw sequencing data were processed by removing reads with an N ratio exceeding 10%, reads composed entirely of A bases, and low-quality reads where over 50% of the bases had a quality score of Q ≤ 20. Clean reads were aligned to the reference genome (*P. yezoensis* GCA_009829735.1) using HISAT2. Based on the HISAT2 alignment results, transcripts were reconstructed with StringTie and all of the expression genes were calculated with RSEM. Differential gene expression was evaluated with DESeq2. Genes with an adjusted $p < 0.05$ and a fold change ≥1.5 were considered statistically significant differentially expressed genes (DEGs). The DEGs were then classified and annotated based on the Kyoto Encyclopedia of Genes and Genomes (KEGG).

2.7. Statistical analyses

Statistical analyses were performed using SPSS 21.0 (SPSS Inc., Chicago, USA). The homogeneity of variance was examined using Levene's test before all statistical analyses. One-way ANOVA was used to establish differences among treatments, and Tukey's test were used to make post hoc comparisons. Differences were considered to be statistically significant at $p < 0.05$.

3. Results

3.1. Radiation conditions

Average irradiances and average daily doses of PAR, UVA, and UVB under each treatment are summarized in Table 1. Under the PAR + UVA treatment, the estimated daily UVA dose was 63.0 kJ m^{-2}, and the biologically effective weighted irradiance for DNA damage was negligible (<0.01 W m^{-2}). Under the PAR + UVR treatment, the daily UVB dose was 2.52 kJ m^{-2}, and the weighted irradiance for DNA damage increased to 0.12 W m^{-2}, indicating a significant genotoxic potential. The weighted irradiance for photoinhibition was 0.23 W m^{-2} under PAR + UVA and 0.31 W m^{-2} under PAR + UVR. These quantitative differences in radiation quality and dose provide a basis for interpreting the subsequent physiological and transcriptomic responses.

3.2. Chlorophyll fluorescence, photosynthesis and respiration rates

As shown in Fig. 1, the presence of UVA (315–400 nm) had no significant effect on the maximum quantum yield of photosystem II (PSII) (F_v/F_m) (One-way ANOVA, $p = 0.476$). In contrast, the presence of UVB (280–315 nm) significantly reduced F_v/F_m from 0.58 to 0.42 (One-way ANOVA, $p < 0.05$) (Fig. 1A). UVB radiation also significantly reduced the net photosynthesis rate (Pn) from 1.8 to 1 mmol CO_2 g^{-1} h^{-1}, representing a decrease of ~44% (One-way ANOVA, $p < 0.05$), but UVA alone showed no significant effect on Pn (One-way ANOVA, $p = 0.379$) (Fig. 1B). On the other hand, the respiration rate was significantly enhanced under PAR + UVA treatment (One-way ANOVA, $p < 0.05$), increasing from 0.77 to 1.28 mmol CO_2 g^{-1} h^{-1}, whereas no significant change was observed between PAR and PAR + UVR treatments (One-way ANOVA, $p = 0.458$) (Fig. 1B).

3.3. Carboxylation and oxidation of Rubisco, carbonic anhydrase and carbon concentrating mechanisms

The catalytic activity of Rubisco involves both carboxylation and oxidation reactions, which are strong related to photosynthetic carbon

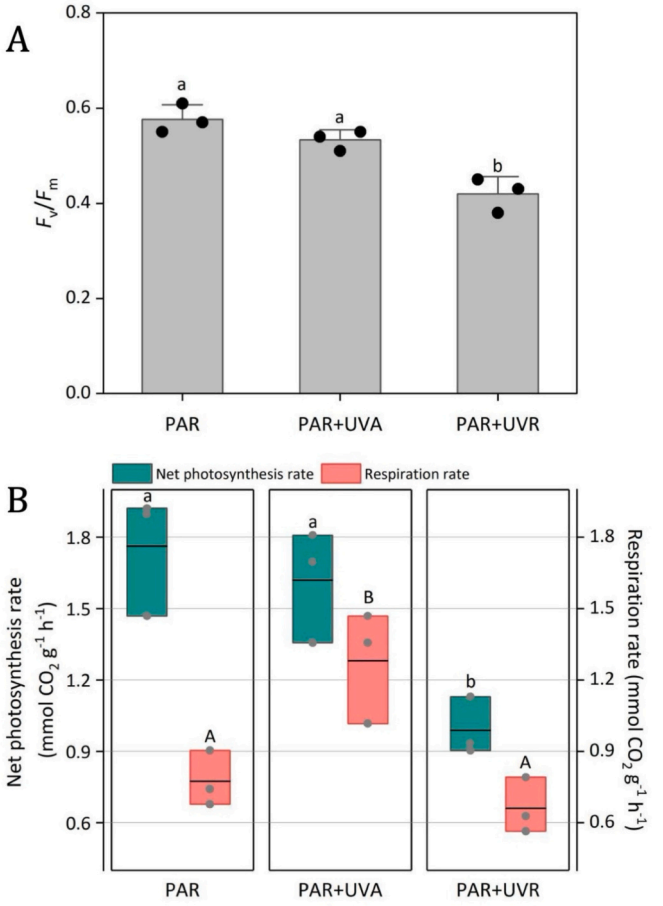

Fig. 1. The maximum quantum yield of PSII (F_v/F_m, panel A), net photosynthesis rate (mmol CO_2 g^{-1} h^{-1}, green bars) and respiration rate (mmol CO_2 g^{-1} h^{-1}, red bars) (panel B) of *P. yezoensis* growing at PAR, PAR + UVA and PAR + UVR conditions. Data are means ± SD ($n = 3$), the dots represent the replicate data, and the different letters above the column indicate a significant ($p < 0.05$, Tukey's test) difference between the treatments. Lowercase and uppercase letters in panel B denote significant differences for net photosynthesis rate and respiration rate, respectively. (For interpretation of the references to colour in this figure legend, the reader is referred to the web version of this article.)

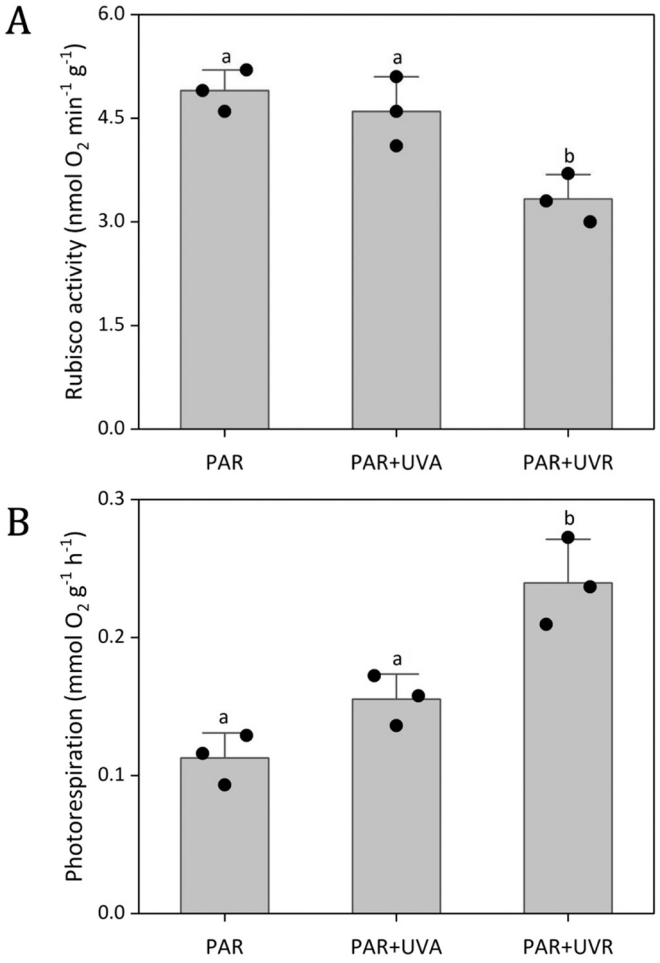

Fig. 2. Rubisco activity (nmol O_2 min^{-1} g^{-1}, panel A) and photorespiration rate (mmol O_2 g^{-1} h^{-1}, panel B) of *P. yezoensis* growing at PAR, PAR + UVA and PAR + UVR conditions. Data are means ± SD (n = 3), the dots represent the replicate data, and the different letters above the column indicate a significant ($p < 0.05$, Tukey's test) difference between the treatments.

assimilation and photorespiratory carbon loss. Similar to Pn, changes of carboxylation of Rubisco also exhibited a significant decrease under the PAR + UVR condition (One-way ANOVA, $p < 0.05$), but showed no significant difference between PAR and PAR + UVA (One-way ANOVA, $p = 0.379$) (Fig. 2A). In contrast, photorespiration was significantly enhanced by PAR + UVR (One-way ANOVA, $p < 0.05$) (Fig. 2B). Given that the balance between carboxylation and oxidation is determined by the availability of CO_2 and O_2 at the active site of Rubisco, we further evaluated the carbonic anhydrase (CA) activities and carbon concentrating mechanisms (CCMs). As shown in Fig. 3A, compared with PAR alone, the half-saturation constant ($K_{0.5}$) for CO_2-dependent photosynthesis was significantly reduced under PAR + UVA treatment (One-way ANOVA, $p < 0.05$), but remained unchanged under PAR + UVR (One-way ANOVA, $p = 0.537$), indicating that CCMs were enhanced by PAR + UVA. Again, the maximal photosynthetic rate (V_{max}) was significantly reduced under PAR + UVR condition (One-way ANOVA, $p < 0.05$), but showed no significant change between PAR alone and PAR + UVA (One-way ANOVA, $p = 0.412$) (Fig. 3A). Moreover, both total and periplasmic CA activities were significantly enhanced under PAR + UVA compared to PAR and PAR + UVR (One-way ANOVA, $p < 0.05$ for both) (Fig. 3B). These results further confirmed the fact that the presence of UVA facilitates the carboxylation of Rubisco.

3.4. Reactive oxygen species, MDA contents and antioxidant enzyme activities

When absorbed energy exceeds the utilization capacity of algae, the resulting excess excitation energy leads to the accumulation of reactive oxygen species (ROS), which are known to induce oxidative stress and damage biomolecules such as pigments, proteins, and lipids. As shown in Fig. 4, both the ROS content and MDA content (Fig. 4A) increased significantly under PAR + UVR conditions (One-way ANOVA, $p < 0.05$ for both), but no significant differences were observed between PAR and PAR + UVA conditions. In response to the elevated oxidative stress, the activities of key antioxidant enzymes, including SOD and CAT (Fig. 4B), showed significant increases under PAR + UVR condition (One-way ANOVA, $p < 0.05$ for both).

3.5. Transcriptional responses

Principal components analysis showed significant differences among PAR, PAR + UVA and PAR + UVR treatments, PC1 contributed 23.8% and PC2 contributed 17.7% of the total variance, respectively (Fig. 5A). A total of 1106, 874 and 260 differentially expressed genes (DEGs) (fold change≥1.5-fold, $p < 0.05$) were identified in the comparisons of PAR + UVA vs. PAR, PAR + UVR vs. PAR and PAR + UVR vs. PAR + UVA, with 892, 539 and 50 up-regulated DEGs and 214, 335 and 210 down-regulated DEGs, respectively (Fig. 5 B). Pathways enrichment analysis

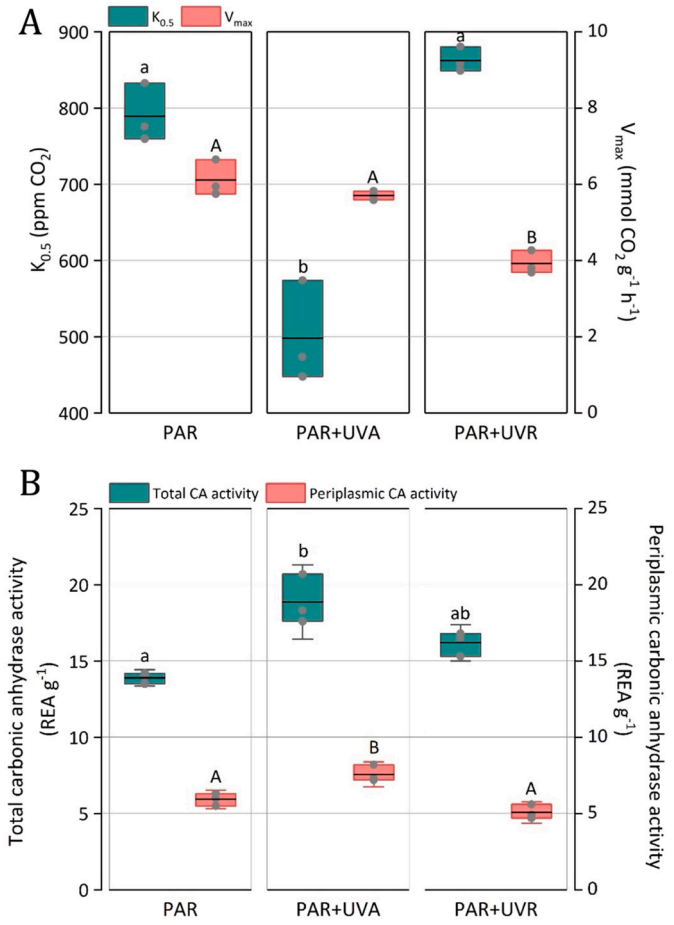

Fig. 3. Values of the half-saturation constant ($K_{0.5}$, the CO_2 concentration that results in half of V_{max}; green bars in panel A), the maximum CO_2-saturated photosynthetic carbon fixation rates (V_{max}, mmol CO_2 g^{-1} h^{-1}, red bars in panel A), the total carbonic anhydrase activity (REA g^{-1}, green bars in panel B) and the periplasmic carbonic anhydrase activity (REA g^{-1}, red bars in panel B) of *P. yezoensis* growing at PAR, PAR + UVA and PAR + UVR conditions. Data are means ± SD (n = 3), the dots represent the replicate data, and the different letters above the column indicate a significant ($p < 0.05$, Tukey's test) difference between the treatments. Lowercase letters denote significance for $K_{0.5}$ and total carbonic anhydrase activity, while uppercase letters denote significance for V_{max} and periplasmic carbonic anhydrase activity. (For interpretation of the references to colour in this figure legend, the reader is referred to the web version of this article.)

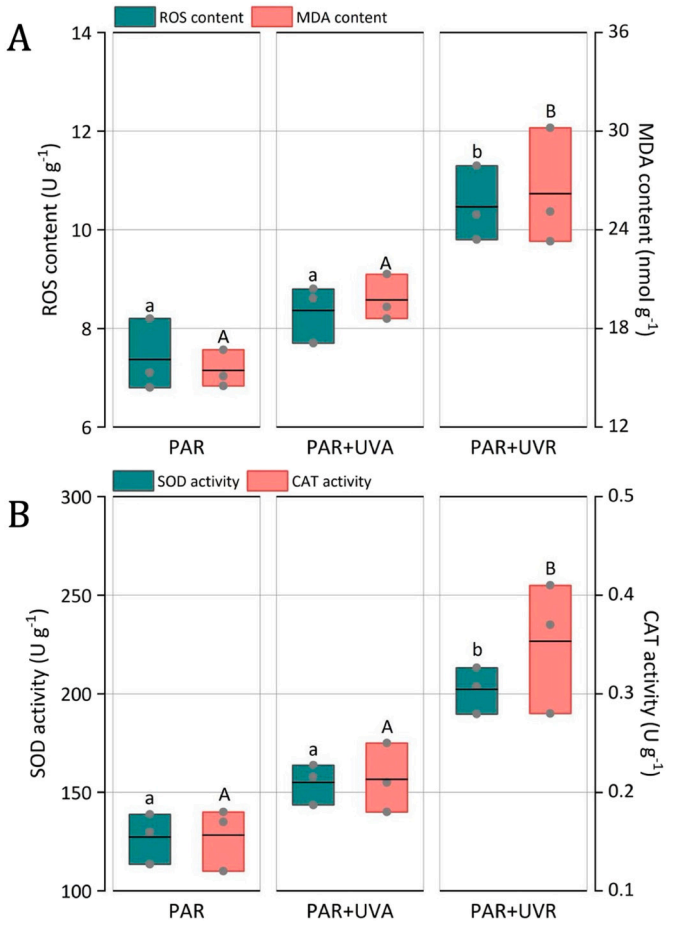

Fig. 4. Contents of the reactive oxygen species (ROS, U g^{-1}; green bars in panel A), and malondialdehyde (MDA, nmol g^{-1}, red bars in panel A), the SOD activity (U g^{-1}, green bars in panel B) and the CAT activity (U g^{-1}, red bars in panel B) of *P. yezoensis* thalli grown at PAR, PAR + UVA and PAR + UVR conditions. Data are means ± SD (n = 3), the dots represent the replicate data, and the different letters above the column indicate a significant ($p < 0.05$, Tukey's test) difference between the treatments. Lowercase letters denote significance for ROS content and SOD activity, while uppercase letters denote significance for MDA content and CAT activity. (For interpretation of the references to colour in this figure legend, the reader is referred to the web version of this article.)

revealed that these DEGs were involved in carbohydrate metabolism, amino acid metabolism, energy metabolism, lipid metabolism, among others (Fig. 5C). Further analysis highlighted several key biological processes, including photosynthesis, carbon metabolism, CCMs, peroxisome-related functions (e.g., antioxidant enzymes), nucleotide excision repair, base excision repair, mismatch repair as well as glutathione metabolism. As shown in Fig. 6A, the expression of light-harvesting antenna proteins, such as *apcC*, *cpcC*, and members of the LHCA1 cluster, was negatively affected by PAR + UVR. A similar down-regulation was also observed for core proteins of PSII, including *psbP* and *psbQ*. In terms of the carbon metabolism, genes associated with carbon fixation, including those related to *tktA*, *FBP*, *FBA* and *GAPDH*, were up-regulated under PAR + UVA and PAR + UVR (Fig. 6B). The enhanced expression of *can* and *cah* genes further indicated increased activity of carbonic anhydrase (Fig. 6B). Consistent with the elevated activities of SOD and CAT, genes involved in antioxidant defense (CAT and SOD), DNA repair process and glutathione metabolism were also up-regulated in both PAR + UVA and PAR + UVR conditions (Fig. 6C, D).

4. Discussion

Intertidal macroalgae are exposed to more extreme diurnally fluctuating conditions than most other plants [30]. Previous studies have shown that UVR can inhibit photosynthesis of both macroalgae via direct and/or indirect ways [2 and references therein]. In our present study, our results demonstrated that attenuated levels of solar UVA enhanced inorganic carbon utilization and carbon concentrating mechanisms, while maintaining photochemical efficiency and avoiding photoinhibition in *Pyropia yezoensis*, which was imprinted in transcriptomic changes.

Solar UVR, especially the irradiance of UVB, is known to reduce both maximum quantum yield of PSII and net photosynthesis rate, inducing damages to PSII integrity and Calvin cycle enzymes [12,19,31–33]. Similarly, we observed a marked downregulation under PAR + UVR conditions in genes encoding light-harvesting antennas (e.g., *cpcC*, *apcC*) and PSII core proteins (e.g., *psbP*, *psbQ*), which aligns with the well-established model of UVB-induced D1 protein degradation and reaction center inactivation documented in both phytoplankton and macroalgae [10,34,35]. While differential impacts of UVB and UVA under

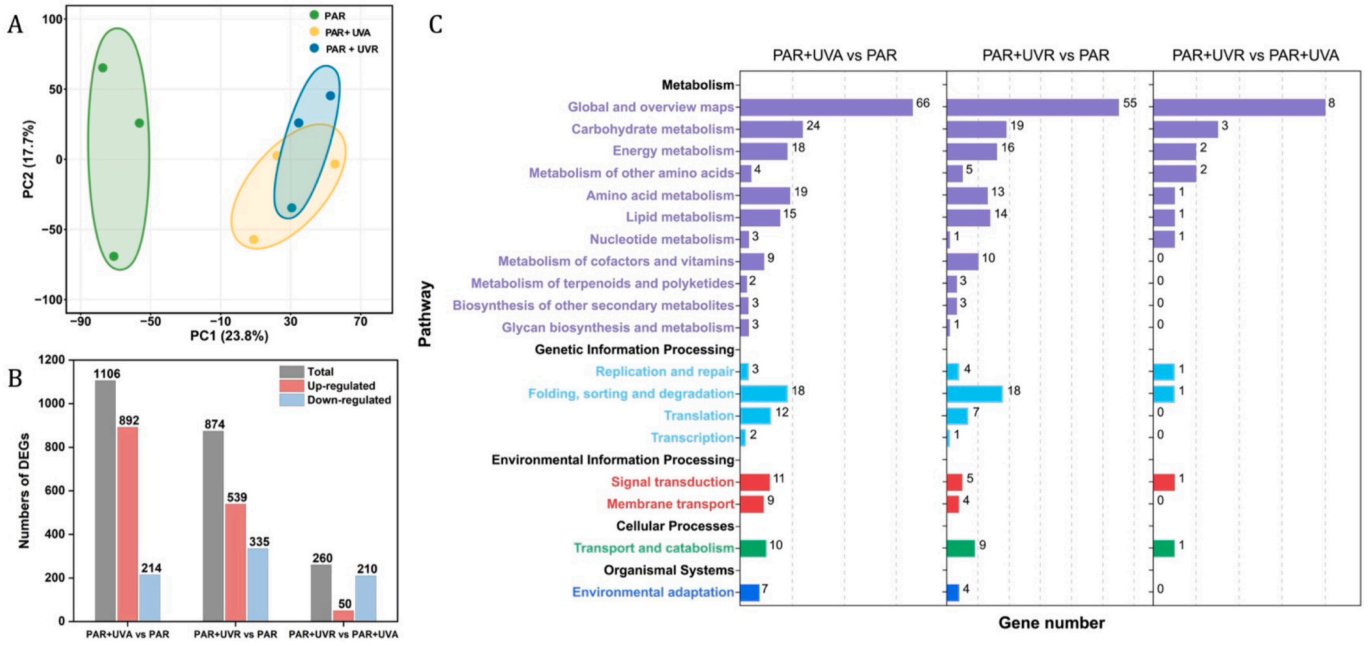

Fig. 5. Transcriptome analysis of *P. yezoensis* thalli grown under PAR, PAR + UVA and PAR + UVR treatments. Panel (A) is the principal components analysis (PCA) of gene expression, panel (B) is the number of differentially expressed genes (DEGs), panel (C) is enriched pathways among different treatments.

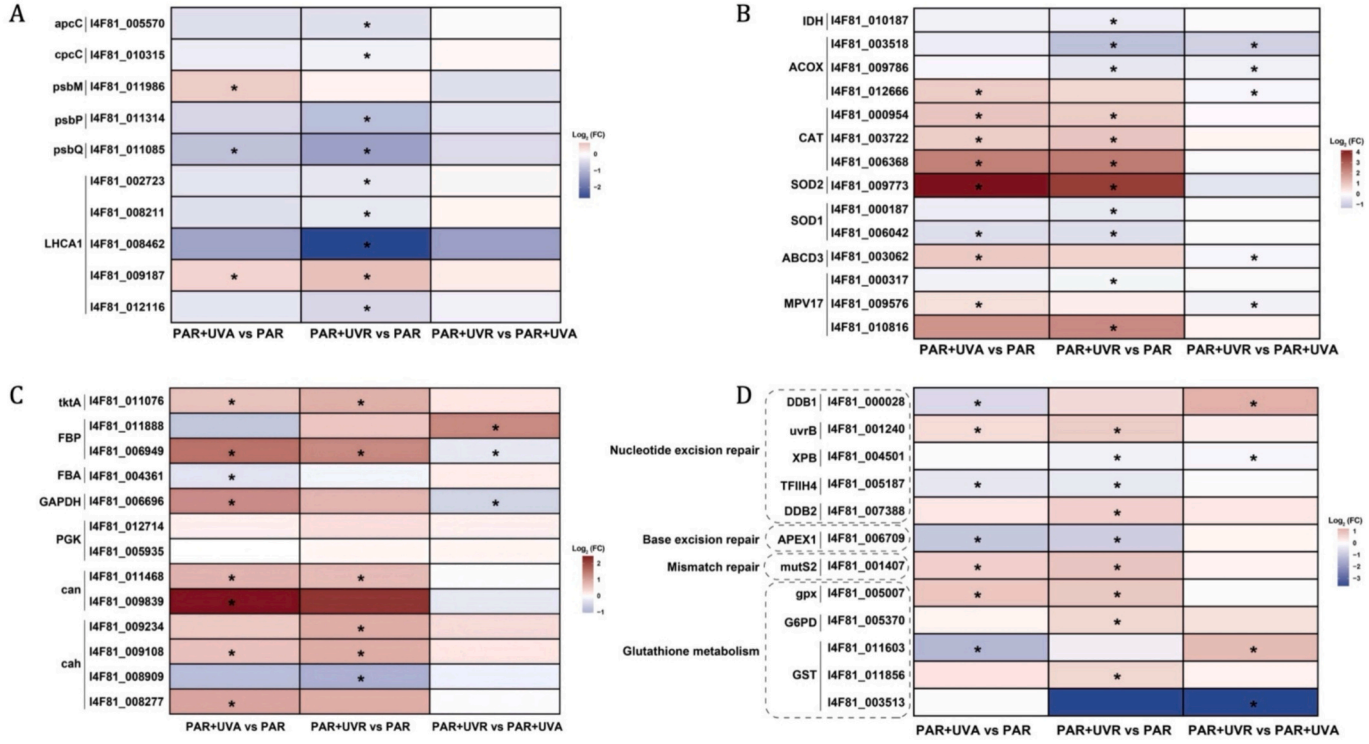

Fig. 6. Heatmaps of significantly altered gene transcripts associated with major KEGG pathways among different treatments. Genes and KEGG pathways shown in different panels are related to the light harvesting antenna and PSII core proteins (panel A), carbon fixation and carbon concentrating mechanisms (panel B), antioxidant defense (panel C) and DNA repair process and glutathione metabolism (panel D), respectively. The symbols "×" indicates a significant ($p < 0.05$, Tukey's test) difference between the treatments.

high levels of solar radiation on macroalgae (see the review by Ji et al. [36] and literatures therein) have been documented, little has been documented on the positive effects of UVR [37,38], especially on the molecular responses. Here, our results from physiological and transcriptomic perspectives demonstrate that UVA enhances inorganic carbon acquisition by up-regulating carbon concentrating mechanisms (CCMs) (Fig. 3A, B, Fig. 6B). Such enhancement of carbon acquisition may contribute to the previously observed UVA-enhanced growth in macroalgae [5,32,38]. However, UVA did not always propel the CA activities in macroalgae. The UVA-enhanced CA activity was only

observed in *Fucus spiralis* rather than *Ulva olivascens* [39]. The different behavior of CA activity is supposed to relate to their different life strategies, where the intertidal algae may rapidly upregulate CA upon re-immersion to compensate for desiccation induced metabolic suppression [39,40]. In addition, the presence of UVA can also enhance nitrate reductase (NR) activity [39], which increase the UVR resilience by prompting carbon and nitrogen metabolism [41,42] and/or by serving as a photoreceptor to absorb UV radiation [43–45]. The transcriptomic data from this work on *P. yezoensis* thereby reveal previously uncharacterized molecular underpinnings of UVA-induced physiological acclimation, highlighting the coordinated upregulation of genes involved in carbon and nitrogen metabolism. In addition to the enhanced carbon acquisition and CCMs, red macroalgae, particularly those of the order Bangiales, possess well-developed photoprotective mechanisms involving mycosporine-like amino acids (MAAs), which function as effective UV-absorbing compounds and antioxidants [46]. MAAs have been extensively documented in *Pyropia* species, where their accumulation is induced by both UV-A and UV-B radiation [47,48]. The observed absence of oxidative stress under PAR + UVA, together with the transcriptomic upregulation of genes related to carbon and nitrogen metabolism, raises the possibility that UVA may also stimulate the synthesis of MAAs, which could contribute to the alleviation of photodamage. This hypothesis is consistent with previous findings that MAAs can scavenge reactive oxygen species and reduce lipid peroxidation [49,50]. Future studies investigating the combined roles of CCMs and MAAs under varying UV regimes would help elucidate the integrated photoprotective strategies employed by intertidal red macroalgae.

Beyond its well-established function in carbon acquisition, CA may also contribute to cellular antioxidant defense by suppressing the formation of ROS through S-glutathione [51–53]. A recent study on *Pyropia haitanensis* showed that CA helps mitigate high-temperature stress through enhanced antioxidant capacity [54]. In the present study, UVA-induced enhancement of CA might have participated in alleviating oxidative damages, since no significant oxidative damages were observed in *P. yezoensis* under PAR + UVA treatment. This is consistent with our previous finding, that increased CO_2 availability alleviate UVR sensitivity in *P. yezoensis* [19,20], most likely due to enhanced carbon assimilation coupled with mitigated stress-induced damages. In contrast, in the presence of UVB, despite the transcriptional upregulation of several CA-related genes (Fig. 6C), CA enzyme activity did not increase (Fig. 3B). This, together with the lower efficient CCMs, likely weaken the Calvin cycle and aggravated the photoinhibition. The significant reduction in V_{max} under PAR + UVR (Fig. 3A) indicates a diminished capacity for CO_2-saturated photosynthetic carbon fixation, which aligns with the downregulation of Calvin cycle-related genes, including *tktA*, *FBP*, and *GAPDH* (Fig. 6B). Together with the reduced Rubisco carboxylation activity (Fig. 2A), these results suggest that UVB suppresses carbon fixation not only by impairing the light-dependent reactions of photosynthesis but also by directly targeting the enzymatic machinery of the Calvin cycle. Consequently, ROS contents in *P. yezoensis* were significantly elevated under PAR + UVR, consistent with documented data that UVR frequently induces oxidative stress in photosynthetic organisms [55–57]. The accumulation of ROS, mainly resulting from excess excitation energy and electron leakage from impaired photosynthetic electron transport chains, is supposed to result in peroxidation of lipids, as indicated by elevated MDA content (Fig. 4A), and potential damage to proteins, nucleic acids, and photosynthetic pigments [58]. These findings are consistent with observations across diverse algal taxa, confirming that UVR, particularly UVB, acts as a key environmental stressor that disrupts cellular redox homeostasis [59,60]. Since positive effects of UVA and negative impacts of UVB of solar radiation can sometime be counterbalanced [61], effects of UVR become invisible [37].

To quantitatively support these findings, we calculated the biologically effective weighted irradiances for photoinhibition [25] and DNA damage [26] based on measured solar spectra and filter cut-offs (Table 1). The weighted irradiance for DNA damage was negligible under PAR + UVA (<0.01 W m^{-2}) but rose to 0.12 W m^{-2} under PAR + UVR, confirming that UVB is the primary driver of genotoxicity and ROS accumulation. The weighted irradiance for photoinhibition was slightly higher under PAR + UVR (0.31 W m^{-2}) than under PAR + UVA (0.23 W m^{-2}). However, despite this measurable value under PAR + UVA, the actual F_v/F_m and Pn showed no significant reduction (Fig. 1). This discrepancy highlights the effectiveness of photoprotective and acclimation mechanisms in *P. yezoensis* under attenuated UVA, including upregulated CCMs, increased CA activity, and likely MAA accumulation [46,62,63]. In contrast, under PAR + UVR, the additional UVB not only increased the weighted irradiance but also directly suppressed Calvin cycle enzymes and induced oxidative stress, leading to clear photosynthetic decline.

Notably, respiration rate was significantly enhanced under PAR + UVA (Fig. 1B), suggesting that the upregulation of carbon acquisition and CCMs may impose increased energy demand. This elevated respiratory activity could partially offset the energy gains derived from enhanced carbon fixation, making the net carbon balance less straightforward than a simple enhancement of photosynthetic output. Although transcriptomic data revealed upregulation of genes involved in carbon metabolism (e.g., *tktA*, *FBP*, *GAPDH*), the concurrent increase in respiration points to a trade-off between carbon acquisition and metabolic costs. In contrast to the elevated respiration under PAR + UVA, respiration rates remained unchanged under PAR + UVR despite pronounced oxidative stress (Fig. 1B). This lack of respiratory response may reflect suppression of mitochondrial activity under severe UVB stress, potentially due to direct damage to mitochondrial electron transport chains or a shift in energy allocation toward immediate repair mechanisms rather than sustained respiration. Alternatively, the uncoupling of respiration from energy demand under UVB stress could indicate a limitation in metabolic flexibility. Similar patterns have been observed in other macroalgae under UVB exposure, where energy metabolism is prioritized for damage repair over maintaining baseline respiratory rates [64]. Together, these differential respiratory responses between UVA and UVB treatments further underscore the contrasting effects of these two UV spectral bands on the metabolic state of *P. yezoensis*.

Under natural intertidal conditions, *P. yezoensis* is subject to drastic environmental changes including solar UVR, desiccation and thermal stresses due to tidal changes. The enhanced CA activity and improved CCMs efficiency observed under PAR + UVA exposure, reported in this study, can only be expected to happen during low light periods without emersion. In the sea-farmed areas, *P. yezoensis* can benefit from solar UVA under cloudy weather or during early morning or late afternoon periods, when UVB is minimal, as UVA enhances inorganic carbon acquisition and CCMs, thereby supporting photosynthetic carbon fixation.

CRediT authorship contribution statement

Di Zhang: Writing – review & editing, Writing – original draft, Visualization, Investigation, Funding acquisition, Data curation, Conceptualization. **Nannan Sun:** Writing – review & editing. **Yonglong Xiong:** Methodology, Data curation. **Kunshan Gao:** Writing – review & editing, Conceptualization.

Declaration of competing interest

The authors declare no competing interests.

Acknowledgements

This study was supported by Shandong Provincial Natural Science Foundation (ZR2022QD134), the National Natural Science Foundation of China (42306139) and the start-up funds from Yantai University (HX22B98).

Appendix A. Supplementary data

Supplementary data to this article can be found online at https://doi.org/10.1016/j.algal.2026.104775.

Data availability

Data will be made available on request.

References

[1] T. Han, Y.S. Han, J.M. Kain, D.P. Häder, Thallus differentiation of photosynthesis, growth, reproduction, and UV-B sensitivity in the green alga *Ulva pertusa* (Chlorophyceae), J. Phycol. 39 (2003) 712–721.

[2] V.E. Villafañe, K. Sundbäck, F.L. Figueroa, E.W. Helbling, Photosynthesis in the aquatic environment as affected by UVR, in: UV Effects in Aquatic Organisms and Ecosystems, The Royal Society of Chemistry, Cambridge, 2003, pp. 357–397.

[3] Y.S. Han, T. Han, UV-B induction of UV-B protection in *Ulva pertusa* (Chlorophyta), J. Phycol. 41 (2005) 523–530.

[4] M.V.F. Giordanino, S.M. Strauch, V.E. Villafañe, E.W. Helbling, Influence of temperature and UVR on photosynthesis and morphology of four species of cyanobacteria, J. Photochem. Photobiol. B Biol. 103 (1) (2011) 68–77.

[5] J. Xu, K. Gao, Use of UV-A energy for photosynthesis in the red macroalga *Gracilaria lemaneiformis*, Photochem. Photobiol. 86 (3) (2010) 580–585.

[6] K. Gao, Y. Zheng, Combined effects of ocean acidification and solar UV radiation on photosynthesis, growth, pigmentation and calcification of the coralline alga *Corallina sessilis* (Rhodophyta), Glob. Chang. Biol. 16 (8) (2010) 2388–2398.

[7] B.E. Henry, K.L. Van Alstyne, Effects of UV radiation on growth and phlorotannins in *Fucus gardneri* (Phaeophyceae) juveniles and embryos, J. Phycol. 40 (3) (2004) 527–533.

[8] H. Jiang, K. Gao, E.W. Helbling, Effects of solar UV radiation on germination of conchospores and morphogenesis of sporelings in *Porphyra haitanensis* (Rhodophyta), Mar. Biol. 151 (5) (2007) 1751–1759.

[9] J. Xu, K. Gao, Photosynthetic contribution of UV-A to carbon fixation by macroalgae, Phycologia 55 (3) (2016) 318–322.

[10] É.C. Schmidt, M. Maraschin, Z.L. Bouzon, Effects of UVB radiation on the carragenophyte *Kappaphycus alvarezii* (Rhodophyta, Gigartinales): changes in ultrastructure, growth, and photosynthetic pigments, Hydrobiologia 649 (1) (2010) 171–182.

[11] K. Ganapathy, K. Chidambaram, R. Janarthanan, R. Ramasamy, Effect of UV-B radiation on growth, photosynthetic activity and metabolic activities of *Chlorella vulgaris*, J. Microbiol. Biotechnol. 6 (2) (2017) 53–60.

[12] K. Gao, J. Xu, Effects of solar UV radiation on diurnal photosynthetic performance and growth of *Gracilaria lemaneiformis* (Rhodophyta), Eur. J. Phycol. 43 (3) (2008) 297–307.

[13] J. Xu, K. Gao, Future CO_2-induced ocean acidification mediates the physiological performance of a green tide alga, Plant Physiol. 160 (4) (2012) 1762–1769.

[14] G. Döhler, Effect of UV radiation on pigments of the Antarctic macroalga *Leptosomia simplex* L, Photosynthetica 35 (3) (1998) 473–476.

[15] M. Altamirano, A. Flores-Moya, F.L. Figueroa, Long-term effects of natural sunlight under various ultraviolet radiation conditions on growth and photosynthesis of intertidal *Ulva rigida* (Chlorophyceae) cultivated in situ, Bot. Mar. 43 (2000) 119–126.

[16] É.C. Schmidt, B. Pereira, R.W. dos Santos, C. Gouveia, G.B. Costa, G.S. Faria, F. Scherner, P.A. Horta, R.P. Martins, A. Latini, F. Ramlov, M. Maraschin, Z. L. Bouzon, Responses of the macroalgae *Hypnea musciformis* after *in vitro* exposure to UV-B, Aquat. Bot. 100 (2012) 8–17.

[17] H. Costa, S.M. Gallego, M.L. Tomaro, Effect of UV-B radiation on antioxidant defense system in sunflower cotyledons, Plant Sci. 162 (6) (2002) 939–945.

[18] W. Wang, Y. Xu, T. Chen, L. Xing, K. Xu, D. Ji, C. Chen, C. Xie, Regulatory mechanisms underlying the maintenance of homeostasis in *Pyropia haitanensis* under hypersaline stress conditions, Sci. Total Environ. 662 (2019) 168–179.

[19] D. Zhang, J. Xu, M. Bao, D. Yan, S. Beer, J. Beardall, K. Gao, Elevated CO_2 concentration alleviates UVR-induced inhibition of photosynthetic light reactions and growth in an intertidal red macroalga, J. Photochem. Photobiol. B Biol. 213 (2020) 112074.

[20] D. Zhang, J. Xu, S. Beer, J. Beardall, C. Zhou, K. Gao, Increased CO_2 relevant to future ocean acidification alleviates the sensitivity of a red macroalgae to solar ultraviolet irradiance by modulating the synergy between photosystems II and I, Front. Plant Sci. 12 (2021) 726538.

[21] C.A. Huffine, R. Zhao, Y.J. Tang, J.C. Cameron, Role of carboxysomes in cyanobacterial CO_2 assimilation: CO_2 concentrating mechanisms and metabolon implications, Environ. Microbiol. 25 (2) (2023) 219–228.

[22] G. Gao, W. Liu, X. Zhao, K. Gao, Ultraviolet radiation stimulates activity of CO_2 concentrating mechanisms in a bloom-forming diatom under reduced CO_2 availability, Front. Microbiol. 12 (2021) 651567.

[23] H. Wu, K. Gao, Ultraviolet radiation stimulated activity of extracellular carbonic anhydrase in the marine diatom *Skeletonema costatum*, Funct. Plant Biol. 36 (2) (2009) 137–143.

[24] J. Beardall, P. Heraud, S. Roberts, K. Shelly, S. Stojkovic, Effects of UV-B radiation on inorganic carbon acquisition by the marine microalga *Dunaliella tertiolecta* (Chlorophyceae), Phycologia 41 (3) (2002) 268–272.

[25] L.W. Jones, B. Kok, Photoinhibition of chloroplast reactions. I. Kinetics and action spectra, Plant Physiol. 41 (6) (1966) 1037–1043.

[26] R.B. Setlow, The wavelengths in sunlight effective in producing skin cancer: a theoretical analysis, Proc. Natl. Acad. Sci. 71 (9) (1974) 3363–3366.

[27] S.v. Von Caemmerer, G.D. Farquhar, Some relationships between the biochemistry of photosynthesis and the gas exchange of leaves, Planta 153 (4) (1981) 376–387.

[28] M. Giordano, S.C. Maberly, Distribution of carbonic anhydrase in British marine macroalgae, Oecologia 81 (4) (1989) 534–539.

[29] M. Björk, K. Haglund, Z. Ramazanov, M. Pedersén, Inducible mechanisms for HCO_3^- utilization and repression of photorespiration in protoplasts and thalli of three species of Ulva (chlorophyta), J. Phycol. 29 (2) (1993) 166–173.

[30] J.J. Bolton, What is aquatic botany? And why algae are plants: the importance of non-taxonomic terms for groups of organisms, Aquat. Bot. 132 (2016) 1–4.

[31] K. Bischof, D. Hanelt, C. Wiencke, Effects of ultraviolet radiation on photosynthesis and related enzyme reactions of marine macroalgae, Planta 211 (4) (2000) 555–562.

[32] Z. Xu, K. Gao, Impacts of UV radiation on growth and photosynthetic carbon acquisition in *Gracilaria lemaneiformis* (Rhodophyta) under phosphorus-limited and replete conditions, Funct. Plant Biol. 36 (12) (2009) 1057–1064.

[33] D. Zhang, S. Beer, H. Li, K. Gao, Photosystems I and II in *Ulva lactuca* are well protected from high incident sunlight, Algal Res. 52 (2020) 102094.

[34] J.N. Bouchard, M.L. Longhi, S. Roy, D.A. Campbell, G. Ferreyra, Interaction of nitrogen status and UVB sensitivity in a temperate phytoplankton assemblage, J. Exp. Mar. Biol. Ecol. 359 (1) (2008) 67–76.

[35] H. Wu, A.M. Cockshutt, A. McCarthy, D.A. Campbell, Distinctive photosystem II photoinactivation and protein dynamics in marine diatoms, Plant Physiol. 156 (4) (2011) 2184–2195.

[36] Y. Ji, Z. Xu, D. Zou, K. Gao, Ecophysiological responses of marine macroalgae to climate change factors, J. Appl. Phycol. 28 (5) (2016) 2953–2967.

[37] M. Wahl, M. Molis, A. Davis, Dobretsov, et al., UV effects that come and go: a global comparison of marine benthic community level impacts, Glob. Chang. Biol. 10 (12) (2004) 1962–1972.

[38] J. Xu, K. Gao, UV-A enhanced growth and UV-B induced positive effects in the recovery of photochemical yield in *Gracilaria lemaneiformis* (Rhodophyta), J. Photochem. Photobiol. B Biol. 100 (3) (2010) 117–122.

[39] B. Viñegla, M. Segovia, F.L. Figueroa, Effect of artificial UV radiation on carbon and nitrogen metabolism in the macroalgae *Fucus spiralis* L. and *Ulva olivascens* Dangeard, Hydrobiologia 560 (1) (2006) 31–42.

[40] A. Flores-Moya, I. Gómez, B. Viñegla, et al., Effects of solar radiation on the endemic Mediterranean red alga *Rissoella verruculosa*: photosynthetic performance, pigment content and the activities of enzymes related to nutrient uptake, New Phytol. 139 (4) (1998) 673–683.

[41] T. Tezuka, F. Yamaguchi, Y. Ando, Physiological activation in radish plants by UV-A radiation, J. Photochem. Photobiol. B Biol. 24 (1) (1994) 33–40.

[42] F.L. Figueroa, B. Viñegla, Effects of solar UV radiation on photosynthesis and enzyme activities (carbonic anhydrase and nitrate reductase) in marine macroalgae from southern Spain, Rev. Chil. Hist. Nat. 74 (2001) 237–249.

[43] M.A. Quiñones, P.J. Aparicio, Flavin type action spectrum of nitrate utilization by *Monoraphidium braunii*, Photochem. Photobiol. 51 (6) (1990) 689–692.

[44] P.J. Aparicio, M.A. Quiñones, Blue light, a positive switch signal for nitrate and nitrite uptake by the green alga *Monoraphidium braunii*, Plant Physiol. 95 (2) (1991) 374–378.

[45] C. Stöhr, U. Glogau, M. Mätschke, R. Tischner, Evidence for the involvement of plasma-membrane-bound nitrate reductase in signal transduction during blue-light stimulation of nitrate uptake in *Chlorella saccharophila*, Planta 197 (4) (1995) 613–618.

[46] J. Vega, G. Schneider, B.R. Moreira, C. Herrera, J. Bonomi-Barufi, F.L. Figueroa, Mycosporine-like amino acids from red macroalgae: UV-photoprotectors with potential cosmeceutical applications, Appl. Sci. 11 (11) (2021) 5112.

[47] N. Korbee, F.L. Figueroa, J. Aguilera, Effect of light quality on the accumulation of photosynthetic pigments, proteins and mycosporine-like amino acids in the red alga *Porphyra leucosticta* (Bangiales, Rhodophyta), J. Photochem. Photobiol. B Biol. 80 (2) (2005) 71–78.

[48] F.L. Figueroa, L. Escassi, E. Perez-Rodrıguez, N. Korbee, A.D. Giles, G. Johnsen, Effects of short-term irradiation on photoinhibition and accumulation of mycosporine-like amino acids in sun and shade species of the red algal genus *Porphyra*, J. Photochem. Photobiol. B Biol. 69 (1) (2003) 21–30.

[49] F. De la Coba, J. Aguilera, F.L. Figueroa, M.V. De Gálvez, E. Herrera, Antioxidant activity of mycosporine-like amino acids isolated from three red macroalgae and one marine lichen, J. Appl. Phycol. 21 (2) (2009) 161–169.

[50] N. Wada, T. Sakamoto, S. Matsugo, Mycosporine-like amino acids and their derivatives as natural antioxidants, Antioxidants 4 (3) (2015) 603–646.

[51] O.V. Polishchuk, Stress-related changes in the expression and activity of plant carbonic anhydrases, Planta 253 (2) (2021) 58.

[52] A. Aspatwar, M.E. Tolvanen, H. Barker, L. Syrjänen, S. Valanne, S. Purmonen, A. Waheed, W.S. Sly, S. Parkkila, Carbonic anhydrases in metazoan model organisms: molecules, mechanisms, and physiology, Physiol. Rev. 102 (3) (2022) 1327–1383.

[53] B.Y. Choi, H. Kim, D. Shim, S. Jang, Y. Yamaoka, S. Shin, T. Yamano, M. Kajikawa, E. Jin, H. Fukuzawa, Y. Lee, The Chlamydomonas bZIP transcription factor BLZ8 confers oxidative stress tolerance by inducing the carbon-concentrating mechanism, Plant Cell 34 (2) (2022) 910–926.

[54] B. Huang, W. Wang, Y. Xu, D. Ji, C. Xie, K. Xu, Extracellular carbonic anhydrases play an important role in the responses of *Pyropia haitanensis* thalli to high-temperature stress, J. Appl. Phycol. (2025) 1–12.

[55] F. Pescheck, K.T. Lohbeck, M.Y. Roleda, W. Bilger, UVB-induced DNA and photosystem II damage in two intertidal green macroalgae: distinct survival strategies in UV-screening and non-screening Chlorophyta, J. Photochem. Photobiol. B Biol. 132 (2014) 85–93.
[56] R. Rautenberger, P. Huovinen, I. Gómez, Effects of increased seawater temperature on UV tolerance of Antarctic marine macroalgae, Mar. Biol. 162 (5) (2015) 1087–1097.
[57] D.T. Pereira, B. Pereira, A. Fonseca, F. Ramlov, M. Maraschin, F. Álvarez-Gómez, F. Figueroa, É. Schmidt, Z. Bouzon, C. Simioni, Effects of ultraviolet radiation (UV-A+ UV-B) on the antioxidant metabolism of the red macroalga species *Acanthophora spicifera* (Rhodophyta, Ceramiales) from different salinity and nutrient conditions, Photochem. Photobiol. 95 (4) (2019) 999–1009.
[58] B. Halliwell, Oxidative damage, lipid peroxidation and antioxidant protection in chloroplasts, Chem. Phys. Lipids 44 (2–4) (1987) 327–340.
[59] D.P. Häder, R.P. Rastogi, UV stress responses in cyanobacteria, in: Ecophysiology and Biochemistry of Cyanobacteria, Springer Nature Singapore, Singapore, 2022, pp. 107–130.
[60] J. Xu, X. Zhao, Y. Zhong, T. Qu, B. Sun, H. Zhang, C. Hou, Z. Zhang, X. Tang, Y. Wang, Acclimation of intertidal macroalgae *Ulva prolifera* to UVB radiation: the important role of alternative oxidase, BMC Plant Biol. 24 (1) (2024) 143.
[61] K. Gao, Y. Wu, G. Li, H. Wu, V.E. Villafane, E.W. Helbling, Solar UV radiation drives CO_2 fixation in marine phytoplankton: a double-edged sword, Plant Physiol. 144 (1) (2007) 54–59.
[62] J. Bonomi-Barufi, F.L. Figueroa, N. Korbee, M.M. Momoli, A.P. Martins, P. Colepicolo, M. Van Sluys, M.C. Oliveira, How macroalgae can deal with radiation variability and photoacclimation capacity: the example of *Gracilaria tenuistipitata* (Rhodophyta) in laboratory, Algal Res. 50 (2020) 102007.
[63] G. Schneider, F.L. Figueroa, J. Vega, P. Chaves, F. Álvarez-Gómez, N. Korbee, J. Bonomi-Barufi, Photoprotection properties of marine photosynthetic organisms grown in high ultraviolet exposure areas: cosmeceutical applications, Algal Res. 49 (2020) 101956.
[64] X. Wang, Y. Zang, S. Xue, S. Shang, J. Xin, L. Tang, J. Chen, X. Tang, Integrated analysis of the physiological, transcriptomic and metabolomic responses of *Neoporphyra haitanensis* after exposure to UV-B radiation: an energy metabolism perspective, Front. Mar. Sci. 11 (2024) 1372252.